Stimulated Brillouin scattering by the interaction between different-order optical and acoustical modes in an As_2Se_3 photonic crystal fiber

Weiqing Gao (高伟清)[1], Liang Chen (陈亮)[1,3], Wenhui Jiang (蒋文辉)[1], Zhengxiong Zhang (张正雄)[1], Xiu Zhang (张秀)[1], Panyun Gao (高攀云)[1], Kang Xie (谢康)[2], Wei Zhang (张维)[1,2,*], Yong Zhou (周勇)[1], Meisong Liao (廖梅松)[3], Takenobu Suzuki (铃木健伸)[4], and Yasutake Ohishi (大石泰丈)[4]

[1]*Department of Optical Engineering, School of Electronic Science & Applied Physics, Hefei University of Technology, Hefei 230601, China*

[2]*School of Instrument Science and Opto-electronics Engineering, Hefei University of Technology, Hefei 230009, China*

[3]*R&D Center of High Power Laser Components, Shanghai Institute of Optics and Fine Mechanics, Chinese Academy of Sciences, Shanghai 201800, China*

[4]*Research Center for Advanced Photon Technology, Toyota Technological Institute, Nagoya 468-8511, Japan*

**Corresponding author: weizhang@hfut.edu.cn*

Received August 30, 2019; accepted October 16, 2019; posted online December 24, 2019

Brillouin gain spectra (BGS) in an As_2Se_3 photonic crystal fiber (PCF) are investigated numerically. The profiles of the BGS are simulated by calculating the characteristics of different-order optical and acoustic waves in the PCFs with different core diameters. For the small-core PCF, there are two peaks in BGS, but there is only one peak for the large-core PCF. We also reveal that in the small-core PCF, the difference of Brillouin frequency shift between the LP_{01} and LP_{11} modes is obvious, while it is not obvious in the large-core PCF. The Brillouin threshold increases with the core diameter increasing.

Keywords: stimulated Brillouin scattering; optical mode; acoustic mode; chalcogenide fiber; photonic crystal fiber.

doi: 10.3788/COL202018.010602.

Stimulated Brillouin scattering (SBS) is a nonlinear process that can be generated in optical fibers[1]. The SBS effect has been studied extensively since it was observed first in 1964[2]. Ippen and Stolen observed SBS in optical fibers in 1972[3]. Then, the SBS effect in optical fibers attracted the attention of researchers and many results have been reported. Many applications of SBS were also investigated on fiber lasers[4–6], fiber amplifiers[7–10], fiber sensors[11,12], and so on. For the applications exploiting the SBS effect, the most gain media were silica fibers. But the silica fibers are not suitable for the SBS effect in the mid-infrared (MIR) waveband because the confinement loss increases sharply after 2 μm. Soft glasses attracted attention because of the wide transmission range and high nonlinear coefficients[13–17]. In 2005, Abedin observed a strong SBS effect in single-mode As_2Se_3 chalcogenide fiber with a Brillouin frequency shift of 7.95 GHz[18]. In 2006, Florea *et al.* obtained the SBS effect in single-mode As_2S_3 and As_2Se_3 fibers[19]. They measured the Brillouin coefficient to be $(3.9 \pm 0.4) \times 10^{-9}$ m/W for the As_2S_3 fiber and $(6.75 \pm 0.35) \times 10^{-9}$ m/W for the As_2Se_3 fiber. Gao *et al.* demonstrated a hybrid Brillouin-erbium fiber laser in a composite cavity with a single-mode tellurite fiber and obtained more than 70 comb lines in 2012[20]. Jain *et al.* investigated erbium-doped tellurite fiber and tellurite photonic crystal fiber (PCF) for the generation of slow light theoretically based on SBS in 2016[21]. They found that the tellurite PCF doped with erbium ions enhanced the maximum allowable power and comparable time delay could be obtained even with reduced PCF length. Recently, Ahmad *et al.* demonstrated a multiwavelength Brillouin fiber laser with Pr^{3+}-doped fluoride fiber[22]. They obtained 36 Stokes lines with a wavelength spacing of 0.16 nm. Usually, the Brillouin gain coefficient decreases with the pump wavelength increasing. So, we may obtain a low Brillouin gain at a long wavelength waveband. In this case, we can design the microstructure of fibers to change the interaction of optical and acoustic fields, resulting in a change of the Brillouin gain coefficient and the profile of the Brillouin spectra. In 2009, Wang *et al.* investigated SBS-based slow light in a microstructure optical fiber (MOF). They obtained a four-times higher time delay efficiency in silica MOF than in single-mode fiber[23]. Mirnaziry *et al.* studied the SBS effect in silicon/chalcogenide slot waveguides in 2016. They found that strong confinement of optical and acoustic modes in the waveguides could lead to a substantial increase in SBS gain[24]. Analysis of the Broullouin gain spectra is an effective way to characterize the SBS effect of fibers with variable microstructures. Full modal analysis of Brillouin gain spectra has been used in variable fibers[25–29], but there are few reports on Brillouin gain spectra analysis in the MIR wavelength.

In this Letter, we investigate the backward Brillouin gain spectra in As_2Se_3 PCFs with 2 μm pump numerically. The profile of the Brillouin gain spectra is studied by

calculating the characteristics of optical and acoustic waves in PCFs. Different gain spectra are simulated by changing the core diameter. We find that there are two peaks in the Brillouin gain spectra for the case of small core PCFs, but for large core PCFs there is only one peak. For the core diameter of 1.16 μm, the frequency difference of the two peaks in the Brillouin gain spectra is 0.505 GHz. By changing the pump optical mode, the influence of the pump mode on the Brillouin gain spectra in backward Brillouin scattering is investigated. The Brillouin frequency shift is different in the small core PCFs from that in the large core PCFs for the optical LP_{01} and LP_{11} modes. The Brillouin threshold increases with increasing core diameter. The reason is analyzed. In small core PCFs, the frequency difference of different acoustic modes is less than that in large core PCFs, which causes the differences of Brillouin gain spectra and threshold between the small core and large core PCFs.

The SBS process can be described as a nonlinear interaction among the pump, the Stokes fields, and the acoustic wave. In the scattering process, the frequencies of the three waves are related by

$$\omega_p = \omega_s + \Omega_B \tag{1}$$

according to the law of energy conservation. The wave vectors are related by

$$k_p = k_s + k_A \tag{2}$$

according to the law of momentum conservation. ω_p, ω_s, and Ω_B are the frequency of the pump, Stokes, and acoustic waves, respectively; and k_p, k_s, and k_A are the wave vector of the pump, Stokes, and acoustic waves, respectively. Here, we consider the backward SBS in optical fibers.

Optical fibers can guide optical waves as well as acoustic waves. Acoustic waves that propagate in optical fibers are governed by the Navier-Stokes equations in an isotropic medium with no external forces as

$$\nabla \cdot (c \nabla u) + \Omega^2 \rho u = 0, \tag{3}$$

where u is the acoustic field, c is the stiffness tensor, ρ is the density of the medium, and Ω is the frequency the acoustic mode. We can get a lot of acoustic modes by solving Eq. (3), and the acoustic modes contribute to the Brillouin gain spectra. In this Letter, we solve a 2-dimensional Navier-Stokes equation to obtain the field distribution of transverse resonant acoustic modes using the finite element method. Then, we use the same method to solve the Helmholtz equation as

$$\nabla^2 E + n^2(\omega') \frac{\omega'^2}{c^2} E = 0 \tag{4}$$

to obtain the optical field distribution, where E is the electric field, n is the refractive index, and ω' is the angular frequency of the optical mode. The modal distributions of both the optical and the ith acoustic field determine the efficiency of the backscattering process according to the overlap integral defined as

$$I_i = \frac{(\int |E|^2 u_i \mathrm{d}x\mathrm{d}y)^2}{\int |E|^4 \mathrm{d}x\mathrm{d}y \int |u_i|^2 \mathrm{d}x\mathrm{d}y}. \tag{5}$$

The overlap integral is calculated in the whole cross section of the fiber and is normalized so that its value is not greater than unity. Previous research indicated that the amplitudes of the different peaks in the Brillouin gain spectra are proportional to the degree of spatial overlap between the field patterns of the interacting acoustic and optical modes[29]. The contribution of each acoustic mode to the Brillouin gain spectra is given by

$$s_B(f) = \sum \frac{\frac{\Delta f_B{}^2}{2}}{(f - f_{B,i})^2 + \frac{\Delta f_B{}^2}{2}} I_i \frac{4\pi n^8 p_{12}{}^2}{\lambda^3 \rho c f_{B,i} \Delta f_B}, \tag{6}$$

where $f_{B,i}$ is the frequency of the Brillouin peak, Δf_B is the full width at half-maximum (FWHM) of the Brillouin gain for each acoustic mode, n is the effective refractive index, p_{12} is the component of the photo-elastic coefficient, λ is the pump wavelength, ρ is the density of the fiber, and c is the speed of light.

Each acoustic mode has a specific field distribution in the cross section of the PCF. The acoustic mode in the backward Brillouin scattering is transmitted along the axial direction of the fiber, which is similar to the field distribution of the light. By solving Eq. (3), the distribution of the acoustic field in the cross section of fiber can be obtained. Brillouin scattering occurs when the wave vector matching condition is satisfied between an acoustic mode and an optical wave. When multiple acoustic modes satisfy the wave vector matching condition, multiple Brillouin scattering occurs at the same time, which results in multipeak Brillouin scattering. In optical fibers, the solution of the acoustic wave usually has multiple modes, which means that for the wave vector of the same optical wave the wave vector of the acoustic modes with different frequencies can satisfy the wave vector matching condition. According to the results, the Brillouin scattering should generally have multiple peaks, but in practical situations, especially in ordinary silica single-mode fibers, the Brillouin scattering spectra is usually a unimodal profile. The reason is that the Brillouin gain is not a single value, but a gain over a certain range. The gain spectra profile can usually be approximated as a Lorentz envelope, and the gain spectral width is usually tens of MHz. If the eigen-frequency difference of multiple acoustic modes participating in Brillouin scattering is small, the multipeak Brillouin scattering is covered by the entire gain spectra. Then, the actual observed result is only one peak. In addition, there may be some higher-order acoustic modes with different acoustic field distributions, but it is not easy to be stimulated simultaneously because the field distribution of these high-order acoustic modes may have less overlap and interaction with the optical fields. So the

multipeak Brillouin gain spectra are not observed. Therefore, for the study of the characteristics of the Brillouin gain spectra in the PCFs, the acousto-optic overlap factor is used to estimate the contribution of each acoustic mode to the Brillouin scattering spectrum. The characteristics of the acoustic mode in the fiber can be controlled by changing the transverse microstructure of the fiber so that different Brillouin gain spectra can be obtained. By investigating the influence of the fiber microstructure on the Brillouin scattering spectra, the suitable PCF can be designed to enhance or suppress the SBS effect in the MIR waveband in the future.

First, the Brillouin gain spectrum by a 2 μm pump in an As_2Se_3 PCF was simulated numerically. The cross section of the As_2Se_3-PCF is shown in Fig. 1. The structure parameters of the As_2Se_3 PCF and the parameters used in the simulation are listed in Table 1. The core diameter $d = 2\Lambda - d_{\text{hole}}$, where d_{hole} is the air hole diameter and Λ is the pitch between adjacent holes. The ratio of d_{hole}/Λ is optimized to be 0.84 to support the LP_{11} mode in the PCF. And the acoustic modes of the PCF can be localized strongly to enhance the Brillouin gain with more air component. The Brillouin gain spectra in the As_2Se_3 PCF with the core diameter of 2.32 μm (calculated according to the hole size in Fig. 1) are shown in Fig. 2.

There are two peaks in the Brillouin gain spectrum with a frequency difference of about 100 MHz Brillouin shift, and the center frequency of the main peak is 6.414 GHz. This result is different from the Brillouin frequency shift of 10 GHz in the most common single-mode silica fiber. It was mainly caused by two aspects. On the one hand, the As_2Se_3 PCF with large air-filling fractions and micron-sized soft-glass cores has a larger refractive-index difference and a higher acoustic-velocity difference between air and glass than those in the silica fibers. On the other hand, the 2 μm pump was used in the calculation. Then, we got the different frequency shifts from the silica fibers.

The two peaks in the Brillouin gain spectra in Fig. 2 are caused by two acoustic modes (L_{01} and L_{02}) with the different eigen frequencies that participated in the Brillouin scattering process. In the case where the wave vector of the LP_{01} mode satisfies the wave vector matching condition with the two acoustic modes, the optical wave is modulated by the two acoustic modes with corresponding different eigen frequencies, and the two Stokes waves generated simultaneously by the acoustic scattering have different frequencies. Then we can find two peaks in the Brillouin gain spectra. The main peak is caused by the interaction between the acoustic L_{01} mode and the optical LP_{01} mode, while the second peak is caused by the interaction between the acoustic L_{02} mode and the optical LP_{01} mode. The number of the Brillouin peaks increases with the core decreasing, which is consistent with the report in Ref. [30].

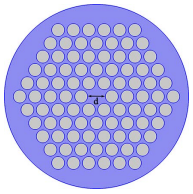

Fig. 1. Cross section of the As_2Se_3 PCF.

Table 1. Parameters of the As_2Se_3 PCF Used in Simulation

ρ ($\text{kg}\cdot\text{m}^{-3}$)	λ (μm)	v_l ($\text{m}\cdot\text{s}^{-1}$)	p_{12}	d (μm)	d_{hole} (μm)	Λ (μm)
4640	2	2250	0.266	1.16	0.84	1
				2.32	1.68	2
				4.76	3.36	4
				6.96	5.04	6
				9.28	6.72	8

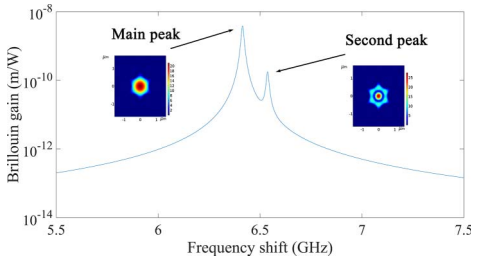

Fig. 2. Brillouin gain spectrum in the PCF with a core diameter of 2.32 μm.

Then, we investigated the Brillouin gain spectrum in the As_2Se_3 PCF with different core diameters to study the affect of core diameter on Brillouin scattering, as shown in Fig. 3.

According to Fig. 3, when the core diameter changes, the Brillouin gain spectrum also has obvious changes. The first change is about the profile of the Brillouin gain spectra. When the core diameter is large, the Brillouin gain spectrum usually has only one peak. When the core diameter decreases to 2.32 μm, two peaks appear in the gain spectrum; when the core diameter decreases to

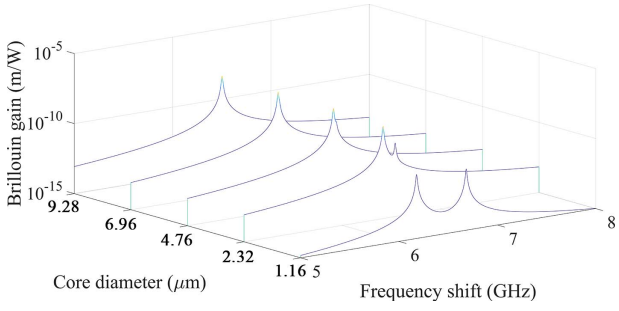

Fig. 3. Brillouin gain spectra in the As_2Se_3 PCFs with different core diameters.

1.16 μm, the frequency interval of the two peaks increases and the peaks increase further. The two peaks in Fig. 3 are still caused by the interaction between the acoustic mode (L_{01} and L_{02}) and the optical mode (LP_{01} mode), which is the same as in Fig. 2. The second change is about the Brillouin gain peak. For the As_2Se_3 PCF with the core diameter of 1.16 μm, the intensities of the two peaks are close, while the intensities are different for the core diameter of 2.32 μm. Although there are many reasons affecting the Brillouin gain peak, the main reason for this phenomenon is that the core is smaller than the pump wavelength. When the core diameter is smaller than the pump wavelength, some of the optical field will leak into the cladding with air holes. Then, for those acoustic field modes confined within the core area, the overlap between the acoustic fields and the optical field will decrease, eventually leading to the decrease in the Brillouin gain peak.

In the As_2Se_3 PCF, the cladding is mainly occupied by air holes, and the acoustic velocity in the air and the glass is different. So the acoustic field distribution in the core is similar to that in the cylindrical acoustic waveguide. We can investigate the acoustic modes in the cylindrical acoustic waveguide instead of PCF. Figure 4 shows the frequency curve with variable diameters of different acoustic modes in a cylindrical acoustic waveguide structure based on As_2Se_3 material. We only solved several low-order acoustic modes. In order to satisfy the wave vector matching conditions of Brillouin scattering, the wave vectors of these acoustic modes are the same. Through the frequency curve in Fig. 4, we can find that when the diameter of the cylinder is small, the eigen frequencies of different acoustic wave modes are different, but when the diameter of the cylinder is large, the eigen frequencies of the acoustic wave modes decrease and have the tendency to arrive at the same eigen frequency. In Brillouin scattering, the Brillouin gain spectrum has a band. When the eigen-frequency difference of different acoustic modes is within the wide range of the gain spectrum, the gain spectrum appears to be with single peak. This is the reason that the As_2Se_3 PCFs with small core diameters exhibit multiple peaks in the Brillouin gain spectra.

Some reports indicate that the pump mode has an effect on SBS[31]. When using a high-order mode pump, the SBS effect may be different from that of the fundamental mode. The differences of the Brillouin gain spectrum between the fundamental mode pump and the LP_{11} mode pump were simulated numerically.

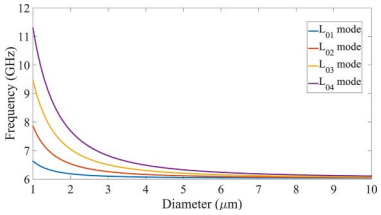

Fig. 4. Frequency curve versus the core diameter for different acoustic modes in a cylindrical acoustic waveguide.

Figure 5(a) shows the Brillouin gain spectra for the pump light with the LP_{01} mode and the LP_{11} mode in the PCF with the core diameter of 2.32 μm. In the As_2Se_3 PCF with the same core diameter, the Brillouin gain spectra generated by the two optical modes have a similar spectral shape. The Brillouin gain spectra by the two pump modes are both bimodal, with only the peak positions shifted. In Fig. 5(a), the higher peak is caused by the interaction between the acoustic L_{01} mode and the optical mode (LP_{01} or LP_{11}), while the lower peak is caused by the interaction between the acoustic L_{02} mode and the optical modes (LP_{01} or LP_{11}). The reason is that the effect of the acoustic waves is more dominant than of the optical waves in the Brillouin gain spectra. When the pump light mode is different, the frequency shift of the Brillouin peaks also changes due to the different propagation constants of different optical modes. It is necessary to satisfy the wave vector matching condition among the pump light, the Stokes light, and the acoustic wave in backward Brillouin scattering. When the propagation constant of the optical wave changes, the acoustic wave vector that satisfies the matching condition also changes, and the eigen frequency of the acoustic wave changes as well. So the Stokes optical frequency generated by the SBS is also different.

The Brillouin gain spectra generated by the same LP_{11} mode pump are also simulated in the As_2Se_3 PCFs with varied core diameters, as shown in Fig. 5(b). It can be found that when the core diameter is small, such as 1.16 μm, the Brillouin gain spectra of different optical modes are different from that in Fig. 3, which can be explained as follows. When the core diameter is large, both the fundamental and the higher-order modes can be confined to the core for optical waves. The effective refractive indices of different modes are different, but this difference is small. When the diameter of the core decreases, the optical field cannot be confined to the core completely, and some of the light will leak into the air-hole cladding through the evanescent wave. The fundamental mode and the higher-order mode are affected by the air holes differently, so the difference of the effective refractive indices of the optical modes will be increased. The difference will affect the Brillouin gain spectra by the wave vector matching condition of Brillouin scattering. The most obvious aspect is the impact on the Brillouin frequency shift.

Through the analysis above, we know that there are many factors affecting the Brillouin gain spectrum. Not

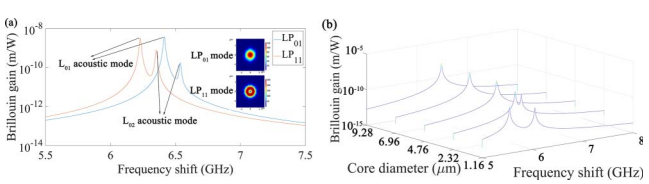

Fig. 5. (a) Brillouin gain spectra by different pump optical modes. (b) Brillouin gain spectra by the LP_{11} optical mode pump.

only the acoustic and optical modes but also the variable core diameters can affect the Brillouin gain spectra. We mainly analyze the specific effects of the core diameter on the SBS effect. The relationship between the frequency shift of the Brillouin main peak and the core diameter under different optical pump modes is presented in Fig. 6(a).

In Fig. 6(a), when the core diameter is different, the Brillouin frequency shift difference produced by the pump with a fundamental mode and a high-order mode is different. When the core diameter is large, the difference of the Brillouin frequency shift between the fundamental mode and the high-order mode pump is small, while the difference increases with the core diameter decreasing. In addition, the Brillouin frequency shift increases with the core diameter for the two optical pump modes of LP_{01} and LP_{11}. There is also an interesting phenomenon. In Fig. 4, the larger the core diameter, the smaller the acoustic wave eigen frequency and the corresponding Brillouin frequency shift are, which seems to be contradictory to the result in Fig. 6(a). In fact, this is not contradictory. In Fig. 4, only the influence of the core diameter on the acoustic field was considered, while the influence of the core diameter on both the acoustic field and the optical field was included simultaneously in Fig. 6(a). The effect of the core diameter on the optical mode can be studied by analyzing the effective refractive indices of the optical fields. Figure 6(b) shows the effective refractive indices of different optical modes as a function of core diameter. According to Fig. 6(b), when the core diameter decreases, the core size will not completely limit the distribution of the optical field gradually, and a part of the light will leak into the air holes so that the effective refractive indices of the optical modes will decrease gradually. The effect of this change on the Brillouin frequency shift can be explained as follows. The effective refractive indices of the optical modes will increase with the core diameter increasing, and the propagation constants of the optical waves will also increase due to the requirements of the wave vector matching condition. Then the acoustic wave vector of Brillouin scattering also needs to be larger. The frequency of the Brillouin scattering acoustic wave also increases because the velocity of acoustic wave in the fiber is mainly determined by the material, not by the core diameter, which causes the Brillouin frequency shift to increase. Then, adding the influence of the core size on the acoustic mode, the result appears like those in Fig. 6(a).

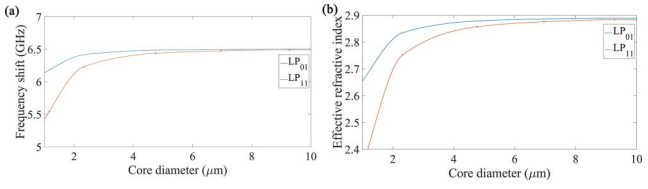

Fig. 6. (a) Brillouin frequency shift versus the core diameter for different optical pump modes. (b) The effective index versus the core diameter for different optical pump modes.

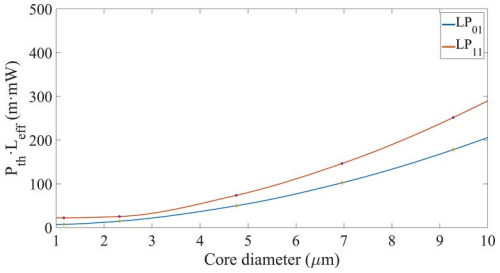

Fig. 7. Product of Brillouin threshold and effective fiber length versus the core diameter.

The Brillouin scattering threshold can be estimated by calculating the Brillouin gain coefficient. The usual Brillouin threshold satisfies the equation as

$$\frac{g_B P_{\text{th}} L_{\text{eff}}}{A_{\text{eff}}} = 21, \tag{7}$$

where P_{th} is the Brillouin threshold power, L_{eff} is the effective fiber length, A_{eff} is the effective mode field area of the optical wave, and g_B is the Brillouin gain factor. The relationship between the Brillouin threshold power and the core diameter is shown in Fig. 7. The longitudinal ordinate in Fig. 7 is the product of the Brillouin threshold power and the effective fiber length. The Brillouin threshold power increases as the core size increases, assuming the effective fiber length is kept constant. For the high-order optical mode pump, the threshold power is higher than that of the fundamental mode pump.

We investigated the backward Brillouin gain spectra in the As_2Se_3 PCFs. First, the profiles of the Brillouin gain spectra were simulated by calculating the characteristics of acoustic waves in As_2Se_3 PCFs. Different gain spectra were obtained by changing the core diameter, and the reasons that the gain spectrum changes with the core diameter were analyzed. We could find that in small core PCFs there are two peaks appearing in Brillouin gain spectra, but for large core PCFs there is only one peak. Then, by changing the pump optical mode, we studied the influence of the pump mode on the Brillouin gain spectra in backward Brillouin scattering. It demonstrated that the pump light mode had a certain influence on the Brillouin gain spectrum, and the effect is not the same as the core diameter of the fiber is different. In the small core PCFs, the Brillouin frequency shift is far different between the LP_{01} mode and LP_{11} mode from those in large core PCFs. Finally, we analyzed the reasons why the core diameter has an influence on the Brillouin gain spectra, and also analyzed the influence of the core diameter on the Brillouin threshold. The result shows that the Brillouin threshold increases when the core diameter increases.

This work was supported by the National Key R&D Program of China (No. 2018YFB0504500), the National Natural Science Foundation of China (NSFC) (Nos. 61875052, 61905059, and 11374084), the Anhui Provincial Natural Science Foundation (No. 1908085QF273), and

the Fundamental Research Funds for the Central Universities (Nos. PA2019GDQT0007 and JZ2019HGTA0037).

References

1. G. P. Agrawal, *Nonlinear Fiber Optics* (Springer, 2013).
2. R. Y. Chiao, C. H. Townes, and B. P. Stoicheff, Phys. Rev. Lett. **12**, 592 (1964).
3. E. P. Ippen and R. H. Stolen, Appl. Phys. Lett. **21**, 539 (1972).
4. G. J. Cowle, Opt. Lett. **21**, 1250 (1996).
5. Y. Luo, Y. Tang, J. Yang, Y. Wang, S. Wang, K. Tao, L. Zhan, and J. Xu, Opt. Lett. **39**, 2626 (2014).
6. X. Heng, J. Gan, Z. Zhang, J. Li, M. Li, H. Zhao, Q. Qian, S. Xu, and Z. Yang, Opt. Lett. **43**, 4172 (2018).
7. G. Gronau and I. Wolff, Electron. Lett. **22**, 554 (1986).
8. N. A. Olsson and J. P. van der Ziel, Appl. Phys. Lett. **48**, 1329 (1986).
9. L. Sheng, D. Ba, and Z. Lü, Chin. Opt. Lett. 1**16**, 111901 (2018).
10. K. Lin, X. Jia, H. Ma, C. Xu, X. Zhang, and L. Ao, Chin. Opt. Lett. **16**, 090604 (2018)
11. H. H. Kee, G. P. Lees, and T. P. Newson, Opt. Lett. **25**, 695 (2000).
12. Bernini, G. Persichetti, E. Catalano, L. Zeni, and A. Minardo, Opt. Lett. **43**, 2280 (2018).
13. K. S. Abedin, Opt. Express **14**, 11766 (2006).
14. G. Qin, H. Sotobayashi, M. Tsuchiya, A. Mori, T. Suzuki, and Y. Ohishi, J. Lightwave Technol. **26**, 492 (2008).
15. X. Zhu and N. Peyghambarian, Adv. Optoelectron. **2010**, 501956 (2010).
16. J. M. P. Almeida, E. C. Barbano, C. B. Arnold, L. Misoguti, and C. R. Mendonça, Opt. Mater. Express **7**, 93 (2016).
17. S. Xing, D. Grassani, S. Kharitonov, L. Brilland, C. Caillaud, J. Trolès, and C.-S. Brès, Optica **4**, 643 (2017).
18. K. S. Abedin, Opt. Express **13**, 10266 (2005).
19. C. Florea, M. Bashkansky, Z. Dutton, J. Sanghera, P. Pureza, and I. Aggarwal, Opt. Express **14**, 12063 (2006).
20. W. Gao, M. Liao, T. Cheng, T. Suzuki, and Y. Ohishi, Opt. Lett. **37**, 3786 (2012).
21. V. Jain, S. Sharma, T. S. Saini, A. Kumar, and R. K. Sinha, Appl. Opt. **55**, 6791 (2016).
22. H. Ahmad, S. N. Aidit, and Z. C. Tiu, Opt. Laser Technol. **99**, 52 (2018).
23. Y. Wang, W. Zhang, Y. Huang, and J. Peng, Opt. Fiber Technol. **15**, 1 (2009).
24. S. R. Mirnaziry, C. Wolff, M. J. Steel, B. J. Eggleton, and C. G. Poulton, Opt. Express **24**, 4786 (2016).
25. N. Shibata, K. Okamoto, and Y. Azuma, J. Opt. Soc. Am. B **6**, 1167 (1989).
26. M. Nikles, L. Thevenaz, and P. A. Robert, J. Lightwave Technol. **15**, 1842 (1997).
27. Y. Koyamada, S. Sato, S. Nakamura, H. Sotobayashi, and W. Chujo, J. Lightwave Technol. **22**, 631 (2004).
28. W. Zou, Z. He, and K. Hotate, IEEE Photonics Technol. Lett. **18**, 2487 (2006).
29. R. Cherif, M. Zghal, and L. Tartara, Opt. Commun. **285**, 341 (2012).
30. P. Dainese, N. Joly, E. J. H. Davies, J. C. Knight, P. St. J. Russell, and H. L. Fragnito, in *Conference on Lasers and Electro-Optics* (2004), paper CThHH3.
31. P. Pradhan, D. Sengupta, L. Wang, C. Tremblay, S. LaRochelle, and B. Ung, Sci. Rep. **7**, 1552 (2017).